

## Tuning the wetting angle of fluorinated polymer with modified nanodiamonds: towards new type of biosensors

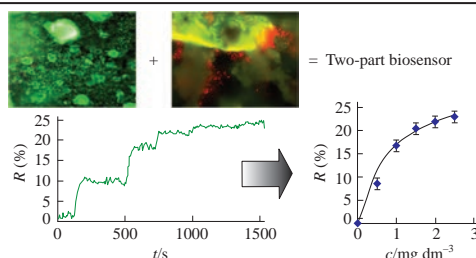
Pavel V. Melnikov,<sup>\*a</sup> Anastasia Yu. Aleksandrovskaya,<sup>a</sup> Alexey V. Safonov,<sup>b</sup> Nadezhda M. Popova,<sup>b</sup> Boris V. Spitsin,<sup>b</sup> Alina O. Naumova<sup>a</sup> and Nikolay K. Zaitsev<sup>a</sup>

<sup>a</sup> M. V. Lomonosov Institute of Fine Chemical Technologies, MIREA – Russian Technological University, 119571 Moscow, Russian Federation. E-mail: melnikovsoft@mail.ru

<sup>b</sup> A. N. Frumkin Institute of Physical Chemistry and Electrochemistry, Russian Academy of Sciences, 119071 Moscow, Russian Federation

DOI: 10.1016/j.mencom.2020.07.015

**A new type of composite oxygen biosensor has been developed. It is based on fine tuning the adhesive and fouling properties of the surface employing modified nanodiamonds with various functional groups. Operability of the sensor has been demonstrated using *Pseudomonas putida* K12 bacteria.**



**Keywords:** nanodiamond, modified nanodiamond, adhesion control, biosensor, whole cell biosensor, BOD, optical sensor, oxygen sensor, fluorinated material.

The development of biosensors and environmental monitoring represent priority trends due to the close relationship between the environment and human health.<sup>1–4</sup> A biosensor is generally composed of a molecule recognition part accompanied by various types of physical or chemical transducers.<sup>5</sup> The materials used for biosensors are divided into three main groups according to the sensing mechanism, namely (i) biocatalytic group comprising immobilized enzymes,<sup>6</sup> (ii) bioaffinity one including antibodies and nucleic acids and (iii) microbe-based one.<sup>7</sup> Examples of the last group are whole cell biosensors with prokaryotic or eukaryotic cells, which typically use respiration to monitor different metabolic events. The respiration represents a fundamental cellular process capable of adapting and responding to physical and chemical changes and thus suitable for analytical signal generation.<sup>8</sup> The related sensors have been used for detection of wastewater contamination,<sup>9</sup> monitoring of fermentation<sup>10</sup> as well as other technological processes.<sup>11</sup> The biochemical oxygen demand (BOD) parameter is employed for monitoring the purity of an aqueous environment<sup>12</sup> and represents the amount of dissolved oxygen required for biochemical oxidation of organic substances contained in a sample at certain temperature over a specific time period. Certain strains or communities of microorganisms are used for rapid assessing BOD and in general the environmental impact.<sup>13</sup> However, for the real assessment of the pollution effect, it is reasonable to employ the unique community of microorganisms inhabited in exactly the investigated body of water.<sup>14,15</sup>

In this work, we have developed a method for formation of specific receptor element *in situ* as well as preparation of reliable reference sensor, which is based on tuning the wettability and fouling of its material surface using modified detonation nanodiamonds (DNDs). The composite material for the optical oxygen sensor was developed earlier<sup>16</sup> and used here as a transducer. An optical type of transduction results in two

advantages, namely lack of oxygen consumption by the sensor and negligible crosstalk between different substances contained in a sample.<sup>8,17</sup> An additional advantage of the composite material employed consists in the linearity of calibration curve, in contrast to purely polymeric sensors characterized by noticeable deviation from linearity.<sup>18</sup>

The preparation of the sensor material as well as optimal conditions were described,<sup>19</sup> for details see Online Supplementary Materials. The sensor consisted of mesoporous SiO<sub>2</sub> microparticles with adsorbed 5,10,15,20-tetrakis(2,3,4,5,6-pentafluorophenyl)porphyrin platinum(II) typically used for the research and commercial oxygen analyzers.<sup>20</sup> The particles were coated with a protective shell of fluorinated surfactant and distributed in fluorine containing polymer Fluoroplast 42, which protected the sensor from the influence of analyzed medium.

Surface properties of the sensor material were tuned using DNDs of three different modifications, namely aminated DND (DND<sub>amine</sub>), chlorinated DND (DND<sub>chl</sub>) and DND with mixed composition (DND<sub>amine+chl</sub>). The details of DND modification and subsequent application onto the surface were described.<sup>21</sup> DND<sub>chl</sub> was synthesized by heating pristine DND in CCl<sub>4</sub>–Ar mixture containing 3% CCl<sub>4</sub> at 400 °C for 5 h.<sup>22</sup> DND<sub>amine</sub> was obtained from DND<sub>chl</sub> by heating in pure ammonia at 300 °C and 1 atm for 2 h. Partially converted product DND<sub>amine+chl</sub> was obtained similarly after 1 h reaction time in ammonia. For uniform application of DNDs on the surface of the material, their suspensions in glycerol were prepared, kept in an ultrasonic bath for 20 min and then immediately applied to the samples with following annealing at 160 °C for 12 h in an Ar atmosphere. For each type of modified DND four different material types were prepared with total particle content on the surface equal to 2.3 × 10<sup>-4</sup>, 3.1 × 10<sup>-4</sup>, 3.8 × 10<sup>-4</sup> and 4.6 × 10<sup>-4</sup> g cm<sup>-2</sup>.

To investigate biofouling, a pure culture of nonpathogenic facultative anaerobic organotrophic bacteria *Pseudomonas*

*putida* strain K12 was used. This strain is known for its ability to form biofilms.<sup>23</sup> Optical visualization of the biofilm was carried out by laser confocal scanning microscopy. Polysaccharide matrix was stained with lectin IV from wheat germ agglutinin (WGA) conjugated with Alexa Fluor 488 fluorescent dye. For the cell visualization, dilute solution of fluorescent dye SYTO 11 in phosphate buffer was used. Images were obtained using an Ar laser at 488 nm for detection of WGA fluorescence and 594 nm for detection of SYTO 11. To locate undyed particles, the Nomarski contrast method was employed (Figure 1). From the obtained images, the percentage of area occupied by cells and polysaccharide matrix was calculated (Figure 2).

Increase in the amount of biofilms and bacterial cells on the surface with an elevation of the content of nanodiamonds is clearly seen, and the observed dependencies coincide with respiratory MTT assay.<sup>21</sup> The highest fouling was revealed for the sample with  $4.6 \times 10^{-4} \text{ g cm}^{-2}$   $\text{DND}_{\text{amine+chl}}$  (see Figure 2), thus  $\text{DND}_{\text{amine+chl}}$  represents a good candidate for the formation of bioreceptor element *in situ*. The sample with  $2.3 \times 10^{-4} \text{ g cm}^{-2}$   $\text{DND}_{\text{amine}}$  demonstrated inhibition of fouling, which is suitable for the reference sensor in a biological environment.

Mechanism of the observed antibacterial action for  $\text{DND}_{\text{amine}}$  seems to resemble the one revealed for polyguanidine derivatives, which are known as antiseptic polycationic polymers.<sup>24</sup> High density of polar groups of the same charge on the DND surface leads to disruption of the cell membrane integrity upon the contact, which results in cell death. In our opinion, the lack of antibacterial action for  $\text{DND}_{\text{amine+chl}}$  originates from mutual charges compensation for functional groups of different polarity on the particle surface. The absence of antibacterial effect for all types of DNDs at their higher content can be explained by increase in wettability of the surface due to the rise in amount of polar groups.<sup>21</sup> The similarity of the results for  $\text{DND}_{\text{amine}}$  and  $\text{DND}_{\text{chl}}$  is caused by a common synthetic route and therefore the same amount of polar groups on their surfaces.

Further, a composite material was prepared with coatings of two types, namely  $4.6 \times 10^{-4} \text{ g cm}^{-2}$   $\text{DND}_{\text{amine+chl}}$  for the receptor itself and  $2.3 \times 10^{-4} \text{ g cm}^{-2}$   $\text{DND}_{\text{amine}}$  for the reference. The material was placed for seven days into a microbiological medium to form biosensor. Then, the readings of the two parts of the sensor were recorded using an optical analyzer.<sup>25</sup> The sensor was placed in saline solution (50 ml) with stirring and then glucose was added stepwise (Figure 3) with further aeration followed by the addition of sodium sulfite at the final step to ensure the correct operation of the oxygen analyzer.

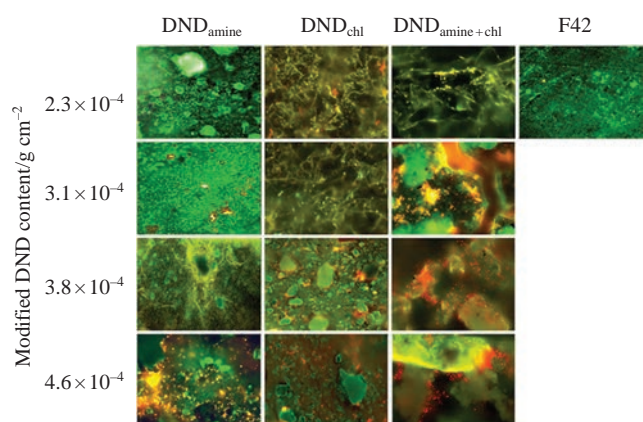


**Figure 1** Polymer sample images (1200 $\times$ ) after incubation at 28  $^{\circ}\text{C}$  for 7 days in a medium with *Pseudomonas putida* K12 and fluorescent staining at different content of modified DND. Substrate material is indicated in green, cells are indicated in yellow, polysaccharide biofilm matrix in orange-red and mucus-coated cells in red, F42 is unmodified Fluoroplast 42 reference.

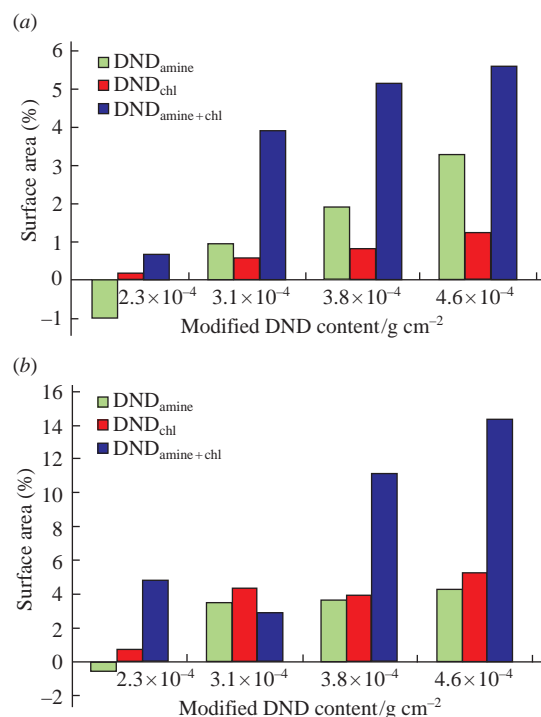


**Figure 2** Surface area fractions (relative to control) occupied by (a) *Pseudomonas putida* K12 cells and (b) polysaccharide matrix for samples with different content of modified DND.

It is seen that the readings of the sensor part coated with  $\text{DND}_{\text{amine}}$  practically do not change with the addition of glucose, demonstrating the values for almost saturated solution. However, the following forced aeration and addition of sodium sulfite result in change in the readings, therefore, the observed output demonstrates the oxygen content in the bulk solution. In contrast, the sensor part coated with  $\text{DND}_{\text{amine+chl}}$  always reveals lower concentration values, responding to glucose additions. This can originate from the respiratory activity of bacterial cells adsorbed on the surface and a local decrease in the oxygen concentration detected by the sensor. Therefore, the biological response value  $R$  represents the difference in the readings of the two sensor parts.

Since receptor elements based on whole microbial cells are actually bioreceptors of the catalytic type, the dependence of  $R$  value on the glucose concentration (see Figure 3, inset) is fit by the following Michaelis–Menten type equation:

$$R = R_{\text{max}}[S]/(K_M + [S]),$$

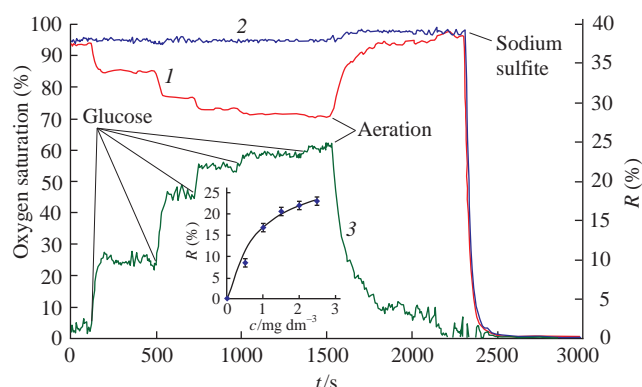


**Figure 3** (1)  $4.6 \times 10^{-4} \text{ g cm}^{-2}$   $\text{DND}_{\text{amine+chl}}$  receptor element response to glucose injections (left axis), (2)  $2.3 \times 10^{-4} \text{ g cm}^{-2}$   $\text{DND}_{\text{amine}}$  reference sensor response (left axis) and (3) the calculated analytical signal  $R$  (right axis). Inset: analytical signal  $R$  vs. glucose concentration.

where  $R_{\max} = 35.5\%$  is the maximal rate of oxygen uptake by immobilized microorganisms achieved at substrate concentration  $[S] \rightarrow \infty$  and  $K_M = 0.87 \text{ mg dm}^{-3}$  is the apparent Michaelis constant, *i.e.* the concentration of substrate at which  $R = R_{\max}/2$ .

In summary, the possibility of optical oxygen biosensor development *via* fine tuning its surface properties has been demonstrated. The sensor was prepared using single base and consisted of two parts, namely the receptor one prone to biofouling and the reference one protected from the fouling. This sensor can be prepared directly in the investigated body of water and then employed to assess substrate specificity or toxic effects utilizing the features of a particular community of microorganisms.

The study was carried out within the framework of the state assignment of the Russian Federation (in accordance with theme no. 0706-2020-0020).

#### Online Supplementary Materials

Supplementary data associated with this article can be found in the online version at doi: 10.1016/j.mencom.2020.07.015.

#### References

- 1 C. I. L. Justino, A. C. Duarte and T. A. P. Rocha-Santos, *Sensors*, 2017, **17**, 2918.
- 2 P. A. Panchenko, A. S. Polyakova, Yu. V. Fedorov and O. A. Fedorova, *Mendeleev Commun.*, 2019, **29**, 155.
- 3 S. A. Gorbатов, M. A. Kozlov, I. E. Zlobin, A. V. Kartashov, I. V. Zavarzin and Yu. A. Volkova, *Mendeleev Commun.*, 2018, **28**, 615.
- 4 N. A. Gavrilenko, T. N. Volgina and M. A. Gavrilenko, *Mendeleev Commun.*, 2017, **27**, 529.
- 5 Q. Gui, T. Lawson, S. Shan, L. Yan and Y. Liu, *Sensors*, 2017, **17**, 1623.
- 6 H. H. Nguyen, S. H. Lee, U. J. Lee, C. D. Fermin and M. Kim, *Materials*, 2019, **12**, 121.
- 7 P. Mehrotra, *J. Oral Biol. Craniofacial Res.*, 2016, **6**, 153.
- 8 N. F. Pasco, R. J. Weld, J. M. Hay and R. Gooneratne, *Anal. Bioanal. Chem.*, 2011, **400**, 931.
- 9 N. Yu. Yudina, V. A. Arlyapov, M. A. Chepurnova, S. V. Alferov and A. N. Reshetilov, *Enzyme Microb. Technol.*, 2015, **78**, 46.
- 10 S. S. Kamanin, V. A. Arlyapov, A. V. Machulin, V. A. Alferov and A. N. Reshetilov, *Russ. J. Appl. Chem.*, 2015, **88**, 463 (*Zh. Prikl. Khim.*, 2015, **88**, 458).
- 11 O. A. Kamanina, D. G. Lavrova, V. A. Arlyapov, V. A. Alferov and O. N. Ponamoreva, *Enzyme Microb. Technol.*, 2016, **92**, 94.
- 12 W. Bourgeois, J. E. Burgess and R. M. Stuetz, *J. Chem. Technol. Biotechnol.*, 2001, **76**, 337.
- 13 V. A. Arlyapov, N. Yu. Yudina, L. D. Asulyan, S. V. Alferov, V. A. Alferov and A. N. Reshetilov, *Enzyme Microb. Technol.*, 2013, **53**, 257.
- 14 M. Buckova, R. Licbinsky, V. Jandova, J. Krejci, J. Pospichalova and J. Huzlik, *Water, Air, Soil Pollut.*, 2017, **228**, 166.
- 15 L. S. B. Upadhyay and N. Verma, in *Environmental Microbial Biotechnology*, eds. L. B. Sukla, N. Pradhan, S. Panda and B. K. Mishra (*Soil Biology*, ed. A. Varma, vol. 45), Springer, 2015, pp. 77–90.
- 16 A. P. Antropov, A. V. Ragutkin, P. V. Melnikov, P. A. Luchnikov and N. K. Zaitsev, *IOP Conf. Ser.: Mater. Sci. Eng.*, 2018, **289**, 012031.
- 17 O. S. Wolfbeis, *BioEssays*, 2015, **37**, 921.
- 18 N. K. Zaitsev, P. V. Melnikov, V. A. Alferov, A. V. Kopytin and K. E. German, *Procedia Eng.*, 2016, **168**, 309.
- 19 P. V. Melnikov, A. O. Naumova, A. Yu. Alexandrovskaya and N. K. Zaitsev, *Nanotechnol. Russ.*, 2018, **13**, 602 (*Rossiiskie Nanotekhnologii*, 2018, **13**, 47).
- 20 M. Quaranta, S. M. Borisov and I. Klimant, *Bioanal. Rev.*, 2012, **4**, 115.
- 21 A. Yu. Aleksandrovskaya, P. V. Melnikov, A. V. Safonov, N. A. Abaturova, B. V. Spitsyn, A. O. Naumova and N. K. Zaitsev, *Nanotechnol. Russ.*, 2019, **14**, 389 (*Rossiiskie Nanotekhnologii*, 2019, **14**, 81).
- 22 B. V. Spitsyn, J. L. Davidson, M. N. Gradoboev, T. B. Galushko, N. V. Serebryakova, T. A. Karpukhina, I. I. Kulakova and N. N. Melnik, *Diamond Relat. Mater.*, 2006, **15**, 296.
- 23 A. Jahn, T. Griebel and P. H. Nielsen, *Biofouling*, 1999, **14**, 49.
- 24 E. Escamilla-García, A. G. Alcázar-Pizaña, J. C. Segoviano-Ramírez, C. Del Angel-Mosqueda, A. P. López-Lozano, E. Cárdenas-Estrada, M. A. De La Garza-Ramos, C. E. Medina-De La Garza and M. Márquez, *Int. J. Microbiol.*, 2017, 5924717.
- 25 N. K. Zaitsev, V. I. Dvorkin, P. V. Melnikov and A. E. Kozhukhova, *J. Anal. Chem.*, 2018, **73**, 102 (*Zh. Anal. Khim.*, 2018, **73**, 73).

Received: 28th January 2020; Com. 20/6116